Molecular Microbiology (2019) 111(1), 187–203

doi:10.1111/mmi.14147
First published online 11 November 2018

Nitric oxide inhibits biofilm formation by *Vibrio fischeri* via the nitric oxide sensor HnoX

Cecilia M. Thompson,[1] Alice H. Tischler,[1] Denise A. Tarnowski,[2,3] Mark J. Mandel[3] and Karen L. Visick [1]*

[1] *Department of Microbiology and Immunology, Health Sciences Division, Loyola University Chicago, Maywood, IL USA.*

[2] *Department of Microbiology-Immunology, Northwestern University Feinberg School of Medicine, Chicago, IL USA.*

[3] *Department of Medical Microbiology and Immunology, University of Wisconsin, Madison, WI USA.*

Summary

Nitric oxide (NO) is an important defense molecule secreted by the squid *Euprymna scolopes* and sensed by the bacterial symbiont, *Vibrio fischeri*, via the NO sensor HnoX. HnoX inhibits colonization through an unknown mechanism. The genomic location of *hnoX* adjacent to *hahK*, a recently identified positive regulator of biofilm formation, suggested that HnoX may inhibit colonization by controlling biofilm formation, a key early step in colonization. Indeed, the deletion of *hnoX* resulted in early biofilm formation *in vitro*, an effect that was dependent on HahK and its putative phosphotransfer residues. An allele of *hnoX* that encodes a protein with increased activity severely delayed wrinkled colony formation. Control occurred at the level of transcription of the *syp* genes, which produce the polysaccharide matrix component. The addition of NO abrogated biofilm formation and diminished *syp* transcription, effects that required HnoX. Finally, an *hnoX* mutant formed larger symbiotic biofilms. This work has thus uncovered a host-relevant signal controlling biofilm and a mechanism for the inhibition of biofilm formation by *V. fischeri*. The study of *V. fischeri* HnoX permits us to understand not only host-associated biofilm mechanisms, but also the function of HnoX domain proteins as regulators of important bacterial processes.

Accepted 1 October, 2018. *For correspondence. E-mail: kvisick@luc.edu; Tel. (708)216-0869; Fax (708)216-9574.

Introduction

Nitric oxide (NO) is a gaseous, readily diffusible molecule with a range of functions in different species (Reiter, 2006; Derbyshire and Marletta, 2009). Eukaryotes utilize low concentrations of NO as a signaling molecule in cell communication (Derbyshire and Marletta, 2009), but can also produce high concentrations that can act as a potent antimicrobial (Fang, 2004). In turn, many bacteria encode proteins to detoxify NO in the environment (Poole *et al.*, 1996; Gardner *et al.*, 2002; Poock *et al.*, 2002; Stevanin *et al.*, 2002; Gardner *et al.*, 2003; Spiro, 2007; Wang *et al.*, 2010b). More recently, endogenous NO production has been observed in bacteria (Crane *et al.*, 2010). NO, either endogenously produced or encountered in the environment, can act as a signaling molecule regulating processes such as biofilm formation, dispersal, motility and quorum sensing (Price *et al.*, 2007; Carlson *et al.*, 2010; Liu *et al.*, 2012; Muralidharan and Boon, 2012; Plate and Marletta, 2012; Henares *et al.*, 2013; Hossain and Boon, 2017).

One bacterium that encounters environmental NO is *Vibrio fischeri*, which is exposed to NO secreted by its symbiotic host, the squid *Euprymna scolopes*. Prior to and during colonization, high levels of NO can be detected in the ducts that lead from the surface of the symbiotic organ to the internal deep crypt spaces, the ultimate site of bacterial colonization. In addition, NO can be found in the mucus secreted on the light organ surface (Davidson *et al.*, 2004). Initial interactions between *V. fischeri* and its host occur in this context: *V. fischeri* forms a bacterial aggregate, or symbiotic biofilm, on the surface of the symbiotic organ from which the bacteria then disperse to enter and ultimately colonize the organ (Nyholm *et al.*, 2000; Visick, 2009). The presence of NO in the mucus restricts the aggregation of nonsymbiotic bacteria during the initial steps of colonization (Davidson *et al.*, 2004).

Previous work identified an NO sensor, named HnoX for *h*eme *n*itric oxide/*o*xygen binding protein, that forms stable Fe(II)–NO complexes (Wang *et al.*, 2010a). HnoX acts

© 2018 John Wiley & Sons Ltd

as an NO sensor that regulates the expression of genes for iron acquisition. An *hnoX* mutant of *V. fischeri* exhibited a competitive advantage over wild-type *V. fischeri* (Wang *et al.*, 2010a), suggesting that HnoX (and NO) modulates the symbiosis between *V. fischeri* and *E. scolopes*. However, it remains unclear how altering the genes for iron acquisition might confer a colonization advantage.

HnoX proteins are often encoded adjacent to a histidine kinase gene and are predicted to inhibit downstream processes regulated by the histidine kinase (Iyer *et al.*, 2003). In *V. fischeri*, HnoX is encoded upstream of the gene for sensor kinase *hahK*, a recently identified positive regulator of biofilm formation (Tischler *et al.*, 2018). HahK controls biofilm formation dependent on the *syp* locus, which encodes proteins that build and export the symbiosis polysaccharide (Syp-PS) (Fig. 1). Syp-PS is a major component of the biofilm matrix (Shibata *et al.*, 2012). In addition to HahK, Syp-PS production is controlled by multiple positive (RscS, SypF and SypG) and negative regulators (BinK, SypF and SypE) (Yip *et al.*, 2006; Hussa *et al.*, 2007; 2008; Morris *et al.*, 2011; Morris and Visick, 2013a; 2013b; Norsworthy and Visick, 2015; Brooks and Mandel, 2016; Pankey *et al.*, 2017; Thompson *et al.*, 2018; Tischler *et al.*, 2018). In the case of the sensor kinase SypF, this regulator was recently shown to control biofilm formation both positively and negatively (Fig. 1). HnoX is predicted to inhibit HahK, and we thus hypothesized that HnoX serves as a negative regulator of biofilm formation.

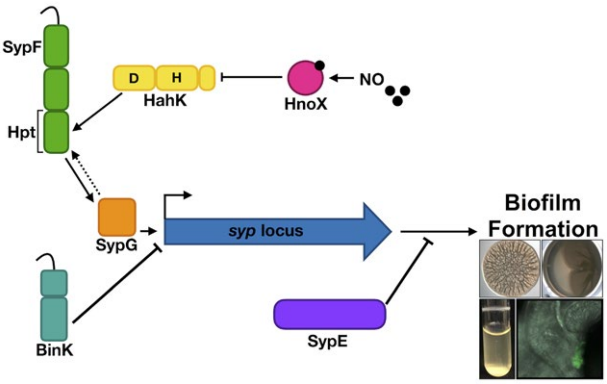

Fig. 1. Model of regulation of biofilm formation by *V. fischeri*. The *syp* locus encodes proteins that build and export the symbiosis polysaccharide (Syp-PS), the major component of the biofilm matrix, resulting in the ability of *V. fischeri* to produce a variety of biofilms, including wrinkled colonies, cohesive cell clumps, pellicles, and symbiotic aggregates. The *syp* locus is a target of control by numerous regulators, including the direct transcriptional activator SypG. SypG is activated by phosphorylation via the sensor kinase protein SypF, which also negatively controls *syp* transcription, likely by dephosphorylation (indicated by the dashed line). RscS (not shown) is another positive regulator that acts through the Hpt domain of SypF to promote *syp* transcription. BinK and SypE negatively control Syp-PS production at the level of *syp* transcription and at a level below *syp* transcription, respectively. HahK is a recently identified positive regulator. In the work presented here, HnoX is identified as a negative regulator that functions via HahK to inhibit *syp* transcription and biofilm formation in the presence of NO. [Colour figure can be viewed at wileyonlinelibrary.com]

Here, we explored the involvement of NO, HnoX and HahK in biofilm formation. Our work reveals HnoX to be a potent inhibitor of biofilm formation and *syp* transcription in the presence of NO. HnoX functions through HahK, which in turn acts upstream of the regulators most proximal to *syp* transcription. Finally, we find that this mechanism is relevant to the animal host, as HnoX also inhibited symbiotic biofilm formation. This work thus identifies both a host-relevant signal that controls biofilm formation and the pathway mediating this control.

Results

HnoX inhibits biofilm formation

Recent work revealed that the sensor kinase HahK promotes biofilm formation by *V. fischeri* (Tischler *et al.*, 2018). Because *hahK* is located downstream of *hnoX*, and because the genes for HnoX/HahK regulatory partners are typically co-transcribed (Iyer *et al.*, 2003), we hypothesized that HahK is negatively controlled by HnoX. If so, then HnoX would negatively regulate wrinkled colony formation, a read-out for biofilm formation. Because wild-type strain ES114 does not form wrinkled colonies (or other *syp*-dependent biofilms) on the standard complex medium (LBS) used to culture this organism, we tested our hypothesis using the strain KV7856. KV7856 readily forms wrinkled colonies due to disruptions of three known negative regulators of biofilm formation, *binK*, *sypE* and *sypF* (See Experimental procedures) (Thompson *et al.*, 2018). Deletion of *hnoX* resulted in precocious biofilm formation: wrinkled colonies formed about four hours earlier than for the parent strain KV7856 (Fig. 2A). Complementation with *hnoX* restored the timing to the level of the parent (Fig. 2A). Similar results were observed using another biofilm-competent strain background (Supp. Fig. 1), indicating that HnoX functions to inhibit wrinkled colony formation.

The *hnoX* mutant exhibited similarly enhanced phenotypes in other assays of biofilm formation. Under static growth conditions, biofilm-proficient strains form pellicles at the air-liquid interface. The biofilm-competent parent strain KV7856 formed weak pellicles at 48 h and displayed robust, cohesive pellicles at 72 h (Fig. 2B). Pellicle formation by the Δ*hnoX* mutant was accelerated, with robust, cohesive pellicles forming by 48 h. Furthermore, the pellicles formed by the Δ*hnoX* mutant, but not its parent, developed wrinkles at 48 h that developed further by 72 h (Fig. 2B). Previously, wrinkling has been observed in pellicles by strains overexpressing a positive regulator of biofilm formation (Ray *et al.*, 2015); the three-dimensional architecture is thought to be a sign

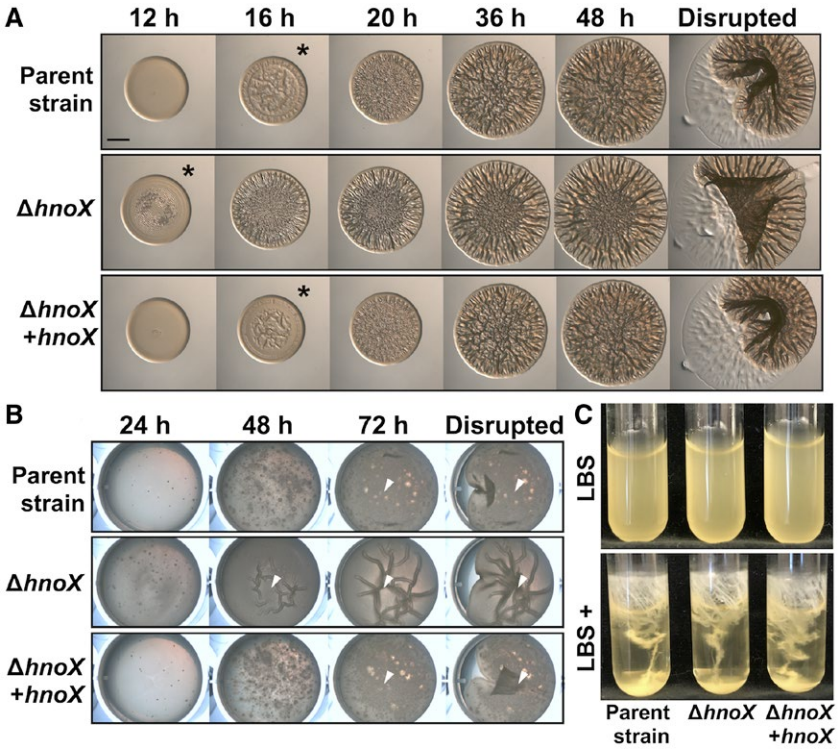

Fig. 2. HnoX inhibits biofilm formation.
A. Development of wrinkled colony morphology was assessed at the indicated time. Asterisks indicate the first time point at which wrinkling was observed. Colonies were disrupted at 72 h to evaluate Syp-PS production. Scale bar indicates 200 μm.
B. Development of pellicles was assessed at the indicated times. At the end of the time course, the pellicles were disrupted with a toothpick to evaluate pellicle strength. Robust pellicle formation is indicated by a white arrow.
C. Representative images of strains grown in shaking cell clumping assays in the absence and presence (+) of calcium were captured after 24 h of incubation. For A, B and C, the following strains were evaluated: Parent strain KV7856; Δ*hnoX* (KV8150); Δ*hnoX* + *hnoX-HA* (KV8175). [Colour figure can be viewed at wileyonlinelibrary.com]

of biofilm maturation. Complementation of the Δ*hnoX* mutant restored both parental timing and appearance of pellicles (Fig. 2B). When grown with shaking in the presence of exogenous calcium, biofilm-competent cells can form macroscopic cell clumping (Tischler *et al.*, 2018) and/or microscopic cell aggregates (Thompson *et al.*, 2018). There was no consistent difference in the timing of macroscopic (Fig. 2C) or microscopic (not shown) cell clumping between the strains, whether in the presence or absence of calcium. Together, these data indicate that *hnoX* is a negative regulator of biofilm formation under different conditions and in two separate genetic backgrounds.

HnoX-mediated inhibition depends on HahK

We probed the HnoX pathway by determining if its activity depended on HahK. We compared biofilm formation by strains deleted for both *hnoX* and *hahK* and, as a control, *hahK* alone. In agreement with previous work describing HahK as a positive regulator of biofilm formation (Tischler *et al.*, 2018), the *hahK* mutant produced minimal wrinkled colony architecture (Fig. 3). Introduction of an epitope-tagged allele of *hahK* restored the parental levels of wrinkling (Supp. Fig. 2). Similarly, wrinkled colony development in the *hnoX-hahK* double mutant was severely diminished and could not be restored by the expression of *hnoX* alone, indicating HahK is epistatic to HnoX. Moreover, while complementation of the double *hnoX-hahK* mutant with both genes restored the parental timing of wrinkling, complementation with *hahK* alone restored precocious wrinkling (Fig. 3). Thus, the enhanced biofilm phenotypes of the *hnoX* mutant depend on HahK.

Because HahK is a putative histidine kinase, we asked if residues predicted to be involved in the autophosphorylation and phosphotransfer, H222 and D506, were required for enhanced *hnoX* mutant biofilms. Despite being expressed (Supp. Fig. 3), neither HahK-H222Q nor HahK-D506A complemented the *hahK* defect (Fig. 4). Similarly, expression of the variants failed to complement the biofilm defect of the *hnoX-hahK* mutant (Fig. 4). Finally, when expressed in a Δ*hnoX* (*hahK*$^{+}$) background, the two HahK variants caused a delay in wrinkled colony formation; this latter result is consistent with the hypothesis that the HahK variants are produced and have an

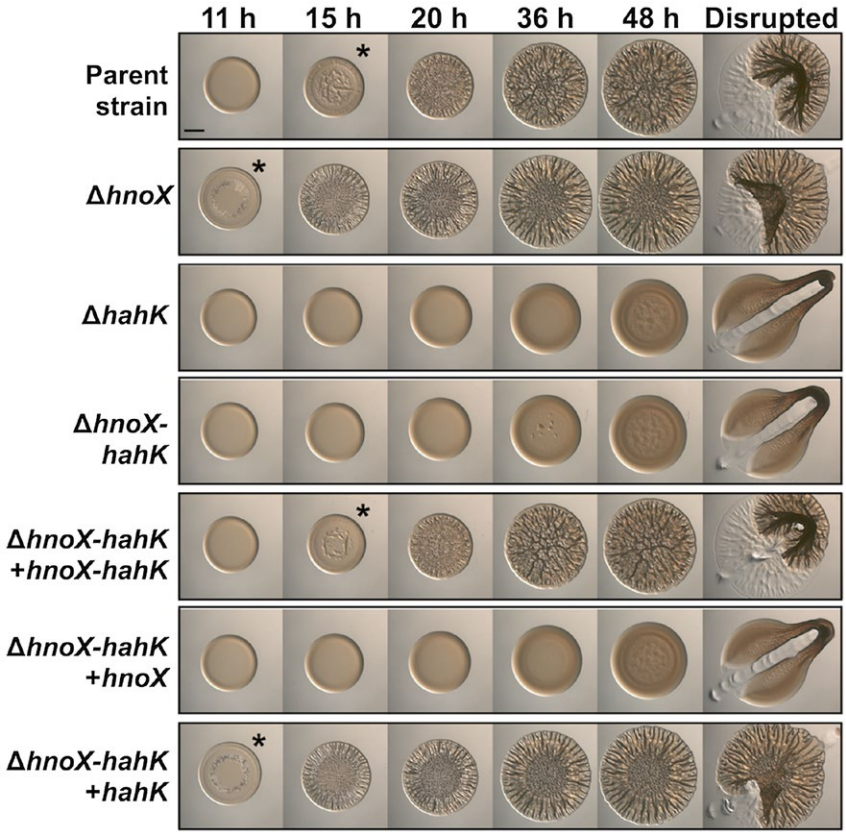

Fig. 3. HnoX-mediated inhibition depends on HahK. Development of wrinkled colony morphology by the following strains was assessed at the indicated time: Parent strain KV7856; Δ*hnoX* (KV8032); Δ*hahK* (KV7956); Δ*hnoX-hahK* (KV8493); Δ*hnoX-hahK* +*hnoX-hahK* (KV8486); Δ*hnoX-hahK* + *hnoX-HA* (KV8494); Δ*hnoX-hahK* + *hahK-HA* (KV8507). Asterisks indicate the first time point at which wrinkling was observed. Colonies were disrupted at 72 h to evaluate Syp-PS production. Scale bar indicates 200 μm. [Colour figure can be viewed at wileyonlinelibrary.com]

activity that disrupts the wild-type HahK biofilm-promoting activity (Fig. 4). These results suggest the enhanced biofilm phenotypes of the *hnoX* mutant depend on the ability of HahK to facilitate phosphotransfer.

HnoX-P114A exhibits increased inhibitory activity

In *Shewanella woodyi*, a substitution of alanine for proline 117 of HnoX results in a mimic of the NO-activated protein that exhibits an increased inhibitory activity and is predicted to inhibit biofilm formation (Muralidharan and Boon, 2012). In *V. fischeri*, the corresponding proline is P115 (Supp. Fig. 4). However, HnoX-P115A failed to alter biofilm formation by the Δ*hnoX* mutant (Fig. 5). The HnoX-P115A variant was detectable by western blot, but at reduced levels (Supp. Fig. 5); thus, unlike the *S. woodyi* protein, the P115A substitution negatively impacts the function and/or the stability of *V. fischeri* HnoX. The *V. fischeri* protein also contains a second adjacent proline, P114. Although this substitution also resulted in decreased protein levels (Supp. Fig. 5), the expression of HnoX-P114A delayed wrinkled colony development by the Δ*hnoX* mutant by 12 h (Fig. 5). Furthermore, the expression of HnoX-P114A in the *hnoX*$^+$ parent delayed wrinkled colony formation by 4 h compared to the *hnoX*$^+$ parent strain expressing the wild-type *hnoX* and delayed wrinkled colony formation by 6 h compared to the *hnoX*$^+$ parent strain, indicating that HnoX-P114A is dominant to wild-type HnoX (Fig. 5). Together, these results suggest that the P114A substitution alters the protein such that it has increased inhibitory activity, potentially similar to the mimic of the NO-bound form of HnoX as seen for *S. woodyi* (Muralidharan and Boon, 2012).

HnoX and HahK control transcription of the syp locus

Production of Syp-PS, the major component of the biofilm matrix, is dependent upon transcription of the *syp* locus. As positive and negative regulators of biofilm formation, HahK and HnoX might regulate biofilm formation at the level of *syp* transcription. Indeed, the *hahK* deletion mutant exhibited low levels of *syp* transcription similar to the biofilm-deficient negative control throughout the time course (Fig. 6A). In contrast, the *hnoX* deletion

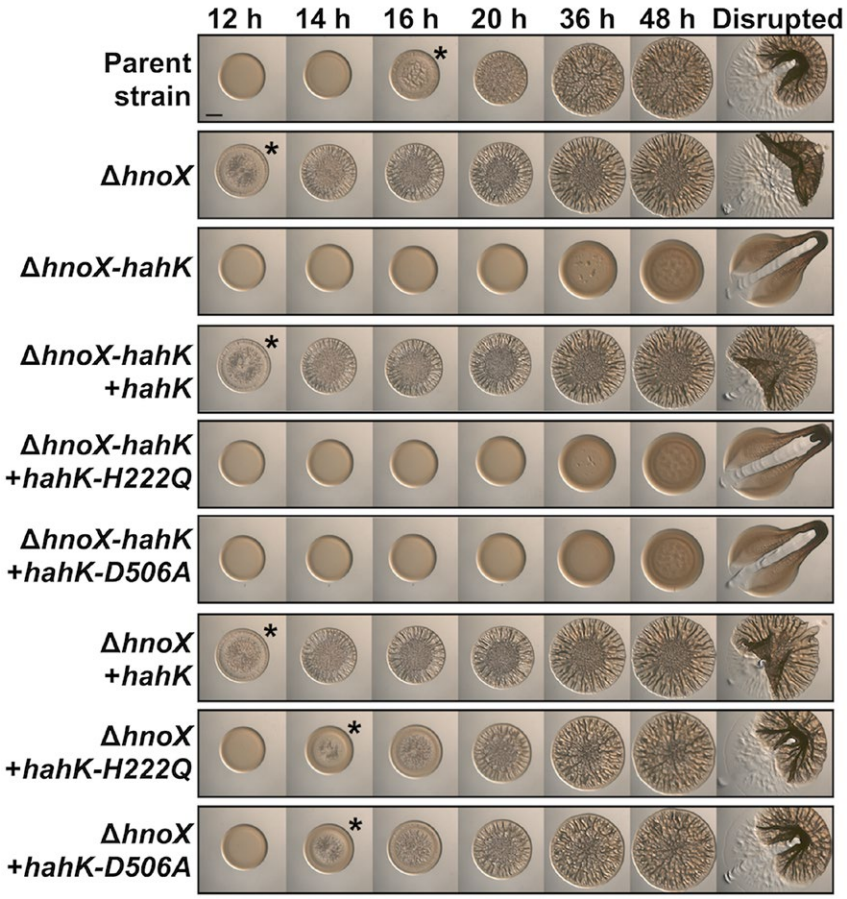

Fig. 4. HahK phosphotransfer mutants fail to promote wrinkled colony formation. Development of wrinkled colony morphology by the following strains was assessed at the indicated time: Parent strain KV7856; Δ*hnoX* (KV8032); Δ*hnoX-hahK* (KV8493); Δ*hnoX-hahK* + *hahK-HA* (KV8507); Δ*hnoX-hahK* + *hahK-H222Q-HA* (KV8504); Δ*hnoX-hahK* + *hahK-D506A-HA* (KV8503); Δ*hnoX* + *hahK-HA* (KV8500); Δ*hnoX* + *hahK-H222Q-HA* (KV8502); Δ*hnoX* + *hahK-D506A-HA* (KV8501). Asterisks indicate the first time point at which wrinkling was observed. Colonies were disrupted at 72 h to evaluate Syp-PS production. Scale bar indicates 200 μm. [Colour figure can be viewed at wileyonlinelibrary.com]

mutant exhibited levels of *syp* transcription similar to the biofilm-proficient positive control (Fig. 6A). Like the *hahK* single mutant, an *hnoX-hahK* double mutant exhibited low levels of *syp* transcription (Fig. 6A), indicating that HahK is epistatic to HnoX.

We wondered if a role for HnoX in controlling *syp* transcription would be more apparent if the cells were grown in the presence of exogenous NO. Indeed, this was the case (Fig. 6B): in the presence of the NO generator Dipropylenetriamine (DPTA)-NONOate, *syp* transcription was completely abrogated in the biofilm-competent parent (*hnoX*$^{+}$) (Fig. 6B). In contrast, *syp* transcription was significantly induced (24-fold) in the absence of *hnoX*, despite the presence of the NO generator (Fig. 6B). This level of induction was similar to that of the *hnoX* mutant grown in the absence of the NO generator (Fig. 6A). These data indicate that NO inhibits *syp* transcription dependent on HnoX. The phenotype of the *hnoX* mutant required *hahK*, as the *hnoX-hahK* double mutant produced low levels of *syp* transcription indistinguishable from the parent and *hahK* single mutant strains (Fig. 6B). Together with the earlier epistasis experiments, these data suggest a pathway in which NO-bound HnoX inhibits *syp* transcription in a manner that depends on HahK-dependent phosphorylation events.

To close the link between HnoX/HahK and *syp* transcription, we evaluated the relationship between these regulators and the two-component regulators, SypF and SypG, that are the most proximal to *syp* transcription (Fig. 1) (Ray *et al.*, 2013; Norsworthy and Visick, 2015). Perhaps not surprisingly, loss of the DNA-binding response regulator SypG disrupted *syp* transcription regardless of the presence or absence of *hnoX* (Fig. 6C). With respect to the sensor kinase SypF, previous work demonstrated that the isolated C-terminal phosphotransferase (Hpt) domain (SypF-Hpt) was sufficient to promote biofilm formation by a biofilm-competent strain if HahK was present (Tischler *et al.*, 2018). We thus hypothesized

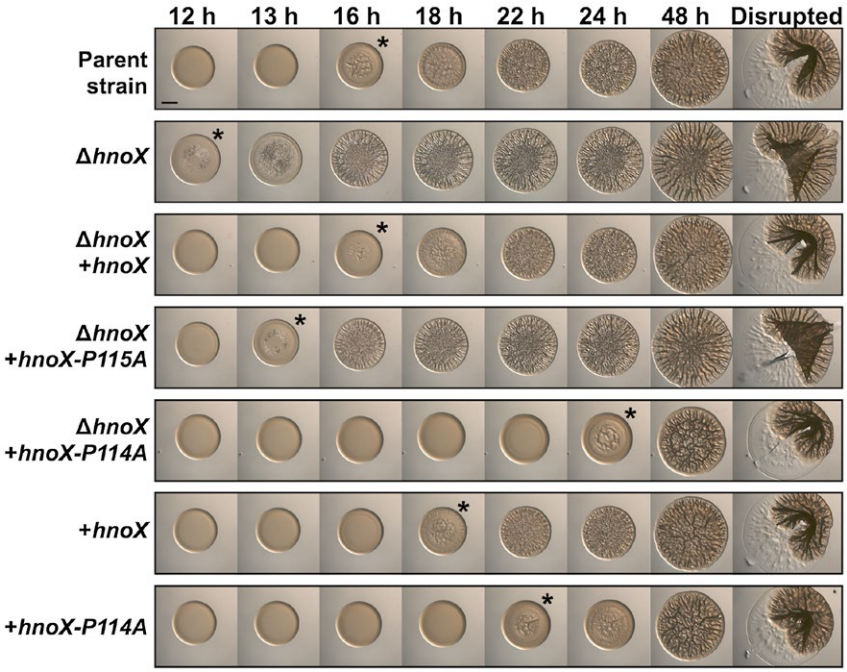

Fig. 5. Identification of an *hnoX* allele with increased activity. Development of wrinkled colony morphology by the following strains was assessed at the indicated time: Parent strain KV7856; Δ*hnoX* (KV8150); Δ*hnoX* + *hnoX-HA* (KV8175); Δ*hnoX* + *hnoX-P115A-HA* (KV8176); Δ*hnoX* + *hnoX-P114A-HA* (KV8177); + *hnoX-HA* (KV8492); + *hnoX-P114A-HA* (KV8487). Asterisks indicate the first time point at which wrinkling was observed. Colonies were disrupted at 72 h to evaluate Syp-PS production. Scale bar indicates 200 μm. [Colour figure can be viewed at wileyonlinelibrary.com]

that the same would be true for *syp* transcription. Indeed, SypF-Hpt-dependent *syp* transcription occurred when HahK was present, but not in its absence (Fig. 6D). Together, these data indicate that HnoX and HahK work upstream of the known *syp* transcriptional regulators to control *syp* transcription (Fig. 1).

Nitric oxide inhibits biofilm formation

In other bacterial systems, it is the NO-bound form of HnoX that inhibits downstream processes (Iyer *et al.*, 2003). Given that *V. fischeri* HnoX binds NO (Wang *et al.*, 2010a) and that NO-exposed cells exhibit decreased *syp* transcription, we predicted that NO would inhibit biofilm formation. We thus tested the impact of NO on biofilms formed in liquid cultures, both static (pellicles) and shaking (macroscopic/cohesive cell clumping), by adding the NO generator, Diethylenetriamine (DETA) NONOate. Addition of 50 μM DETA-NONOate prevented pellicle formation, while lower concentrations (3 μM) diminished pellicle formation (Fig. 7A). Similarly, addition of as little as 25 μM of DETA-NONOate abrogated the ability of biofilm-competent *V. fischeri* to form cohesive cellular clumps; the cultures remained turbid under these conditions (Fig. 7B). Even at the highest concentrations evaluated, the growth of *V. fischeri* was not substantially impaired (Supp. Fig. 6). Together, these data indicate that the biologically relevant signal NO inhibits biofilm formation by *V. fischeri*.

Nitric oxide inhibition depends on HahK and HnoX

We predicted that if NO functions to control biofilm through HnoX, then a *hnoX* mutant should fail to respond to NO addition. Indeed, pellicles formed by the *hnoX* mutant were similar in the presence and absence of low concentrations of an NO generator (Fig. 7C). While the addition of the NO generator abrogated the calcium-induced cell clumping by the biofilm-competent parent strain, it had no impact on the Δ*hnoX* strain grown under the same conditions (Fig. 7D). Even at high DETA-NONOate concentrations, the Δ*hnoX* strain formed robust rings and clumps (Fig. 7D). Complementation of Δ*hnoX* with wild-type *hnoX* diminished pellicle formation and restored turbidity to shaking cultures in the presence of the NO generator (Fig. 7E and F). Complementation of Δ*hnoX* with *hnoX-P114A* also restored turbidity to cultures in the presence of the NO generator, suggesting that the HnoX variant remains responsive to NO (Supp. Fig. 7). Finally, strains defective for both *hnoX* and *hahK* exhibited reduced biofilm formation that was unaffected by the addition of the NO generator (Supp. Fig. 7). Together, these results indicate that NO mediates the inhibition of Syp-dependent

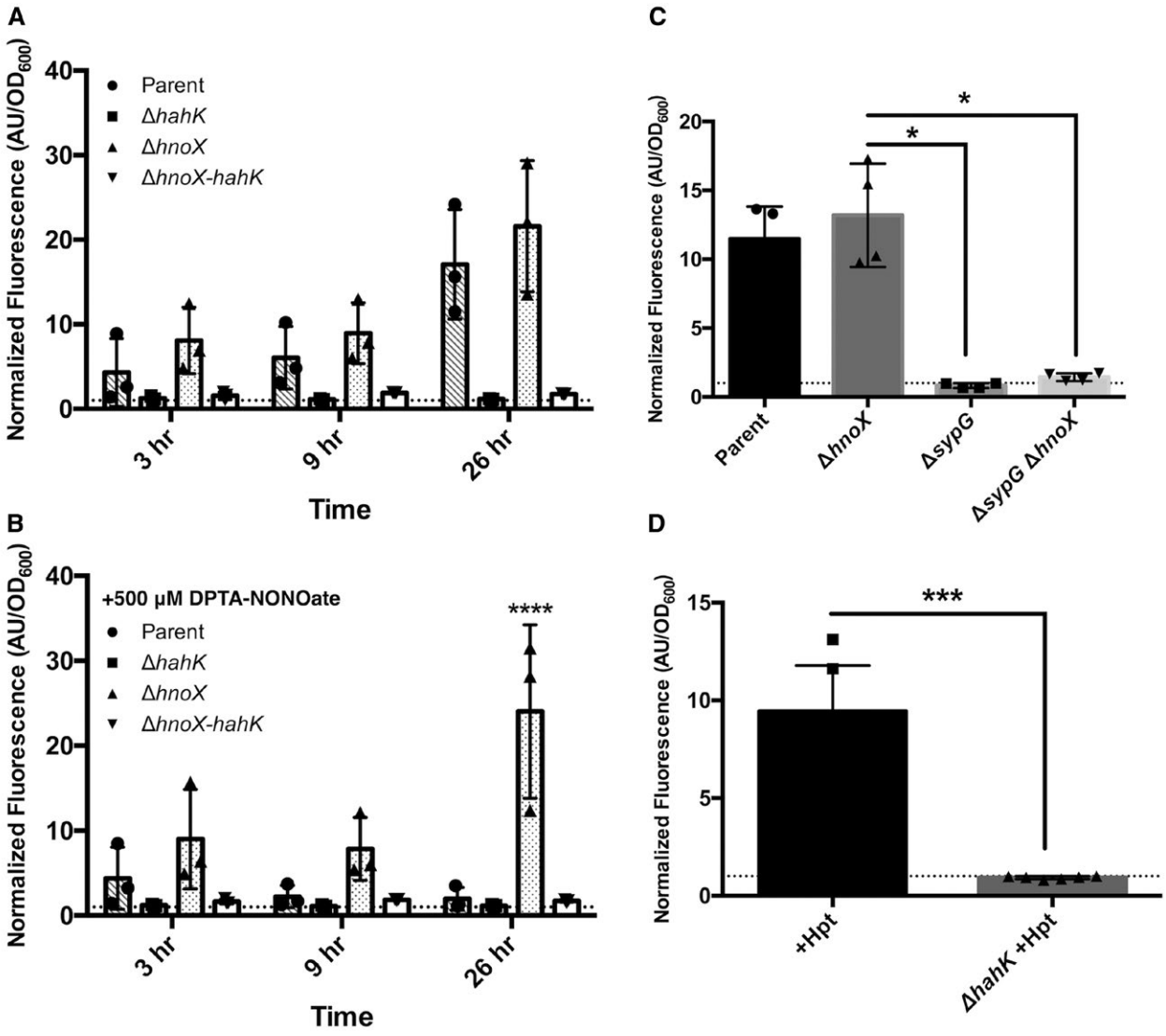

Fig. 6. HnoX and HahK control *syp* transcription. Strains expressing a P*sypA-GFP* reporter (pLL3) were grown overnight at 24°C. Strains were subcultured the next day at an OD_{600} = 0.05. The fluorescence and OD were measured at the indicated time points. The fluorescence/OD600 for each strain was normalized to a biofilm (–) strain (indicated by the dotted line) to generate the normalized fluorescence.
A and B. The strains are as follows: biofilm (+) parent KV7856; Δ*hahK* (KV7956); Δ*hnoX* (KV8150; Δ*hnoX-hahK* (KV8493). Strains were normalized against KV8055. The data were analyzed using a two-way ANOVA, (****$p \leq 0.0001$). Cells were grown in the absence (A) or presence (B) of 500 μM of the NO generator DPTA-NONOate, which was supplemented at the 3 h time point.
C. Strains are as follows: Parent (KV7856), Δ*hnoX* (KV8150), Δ*sypG* (KV8607) and Δ*hnoX* Δ*sypG* (KV8611), normalized against KV6567. The data were analyzed by a one-way ANOVA (*$p \leq 0.05$).
D. Strains are as follows: Δ*sypF* +Hpt (KV8086) and Δ*hahK* Δ*sypF* +Hpt (KV8107), normalized against KV6439. The data were analyzed by a one-way ANOVA (***$p \leq 0.001$).

biofilm pellicles and clumps through the HnoX-HahK regulatory pathway.

HnoX inhibits symbiotic biofilm formation

Previous evidence demonstrated that an *hnoX* mutant outcompeted the wild-type strains for colonization (Wang *et al.*, 2010a), and our results indicate that *hnoX* functions as a negative regulator of biofilm formation. One hypothesis is that an *hnoX* mutant colonizes more efficiently because it forms a better biofilm. To test this possibility, juvenile, aposymbiotic squid were exposed to approximately 3×10^6 of bacteria for 3 h and the symbiotic biofilms (aggregates) formed by Δ*hnoX* cells were measured and compared to *hnoX*$^+$ aggregates. The *hnoX* mutant formed aggregates that consisted of a significantly larger surface area compared to the *hnoX*$^+$ control ($p = 0.0002$) (Fig. 8). These results suggest that *hnoX* negatively regulates symbiotic biofilms, which may account, at least in part, for the colonization advantage of an *hnoX* mutant.

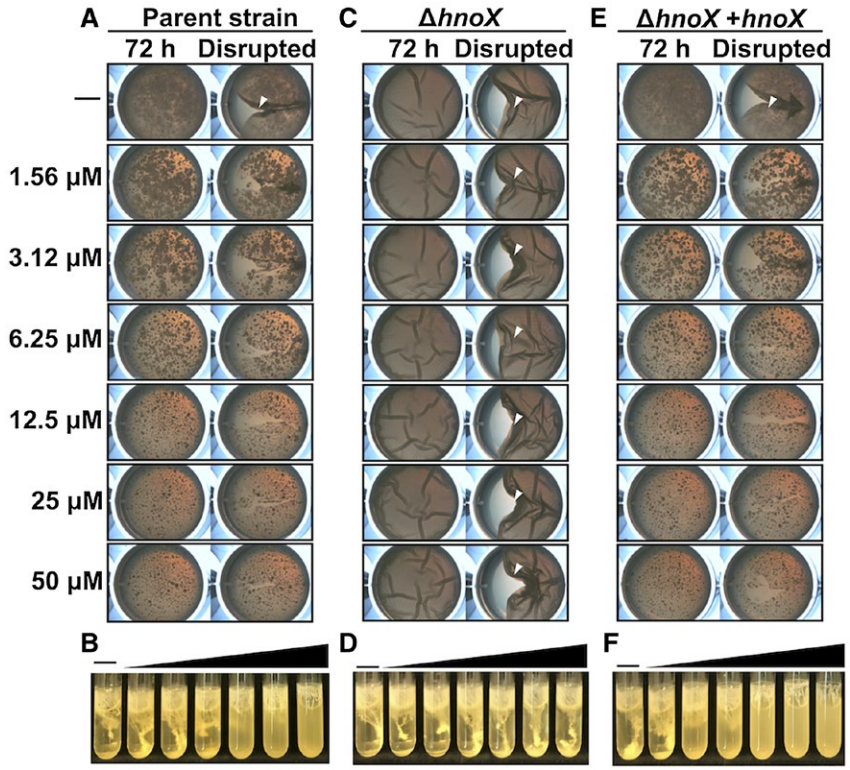

Fig. 7. Nitric oxide inhibition depends on HahK and HnoX.
A, C and E. Development of pellicles was assessed at the indicated time. The NO generator DETA-NONOate was supplemented at the indicated concentrations. The negative control (-) contained the equivalent volume of water. At the end of the time course, the pellicles were disrupted with a toothpick to evaluate pellicle strength. Robust pellicle formation is indicated by a white arrow.
B, D and F. Representative images of strains grown in shaking cell clumping assays in the presence of calcium were captured after 24 h of incubation. The NO generator DETA-NONOate was supplemented at the same concentrations indicated in (A). For pellicle and cell clumping assays, the following strains were assessed for biofilm formation: parent strain KV7856, Δ*hnoX* (KV8150) and Δ*hnoX* + *hnoX-HA* (KV8175).
[Colour figure can be viewed at wileyonlinelibrary.com]

Discussion

V. fischeri employs numerous regulators to control biofilm formation. A series of two-component regulators feed in to positively control production of Syp-PS, a major component of the *V. fischeri* biofilm, via *syp* transcription (Fig. 1) (Yip *et al.*, 2006; Hussa *et al.*, 2007; 2008; Norsworthy and Visick, 2015; Thompson *et al.*, 2018; Tischler *et al.*, 2018). In addition, two negative regulators have been identified that regulate transcription of the *syp* locus (Brooks *et al.*, 2016; Pankey *et al.*, 2017; Thompson *et al.*, 2018; Tischler *et al.*, 2018), and one that posttranscriptionally regulates Syp-PS production (Morris *et al.*, 2011; Morris and Visick, 2013a; 2013b). Despite the plethora of two-component regulators, proteins that sense and respond to environmental signals, the signals that are recognized by these proteins to control biofilm formation, are unknown. Here, we identify a host-relevant signal, NO, that controls *syp* transcription and *syp*-dependent biofilm formation, and the corresponding signal transduction pathway.

NO is an important signaling molecule in mammals (Fang, 2004), and more recently has been implicated in bacterial processes such as quorum sensing, biofilm formation and dispersal (Price *et al.*, 2007; Carlson *et al.*, 2010; Liu *et al.*, 2012; Muralidharan and Boon, 2012; Plate and Marletta, 2012; Henares *et al.*, 2013; Hossain and Boon, 2017). Some bacteria produce endogenous NO, but whether *V. fischeri* does so has not been reported. NO was identified as a defense molecule in the *Vibrio*-squid symbiosis: the squid secretes NO-containing mucus, which serves as the substrate for aggregation, or symbiotic biofilm formation, by *V. fischeri* (Nyholm *et al.*, 2002; Davidson *et al.*, 2004). Inhibitors of NO increased the aggregate formation by symbionts as well as nonsymbionts (Davidson *et al.*, 2004), suggesting that squid-produced NO may generally inhibit biofilm formation. However, no role for NO in controlling *V. fischeri* biofilms had been described previously, nor has the mechanism by which NO might impact biofilm formation been reported.

An insight into the role of NO in symbiosis came with the identification of HnoX, an NO sensor in *V. fischeri* (Wang *et al.*, 2010a). An *hnoX* mutant exhibited a colonization advantage compared to the wild-type cells, leading to the

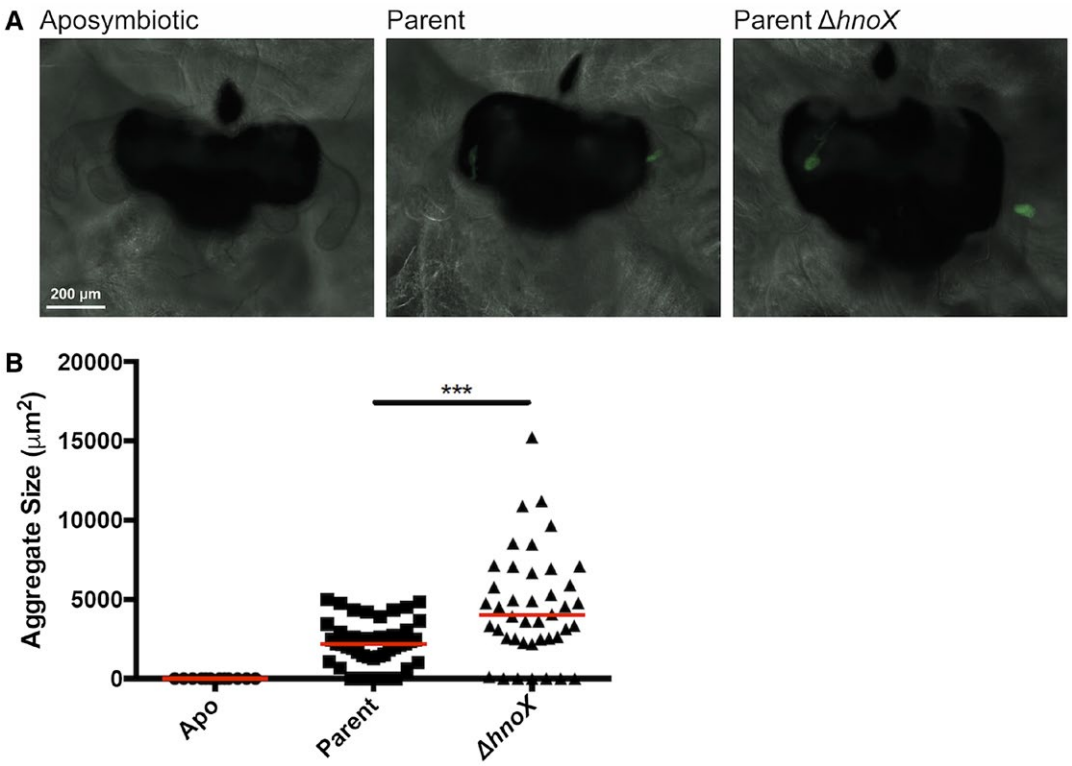

Fig. 8. HnoX inhibits symbiotic aggregation.
A. Aggregates at the entrance to the light organ were visualized at 3 h in either aposymbiotic juveniles or those inoculated with pVSV102-containing parent strain (KV3299) or the Δ*hnoX* derivative (KV8027).
B. Aggregate area was plotted for each inoculation condition as indicated above. Red lines indicate median. Samples were analyzed using a Mann-Whitney test ($p < 0.0001$, $p = 0.0002$); asterisks indicate significance between parent and Δ*hnoX* strains. [Colour figure can be viewed at wileyonlinelibrary.com]

hypothesis that HnoX senses NO and in response coordinates the detoxification of NO during colonization. HnoX does not induce expression of enzymes that neutralize NO, but rather HnoX alters the expression of the genes for iron acquisition. HnoX also suppresses the ability of cells to grow on hemin as the sole iron source in response to NO (Wang *et al.*, 2010a). It was postulated that HnoX suppresses hemin accumulation to prevent an increase in intracellular iron that would lead to the generation of hydroxyl radicals through the Fenton reaction. However, the inability to uptake iron negatively impacts symbiont persistence in the light organ (Graf *et al.*, 1994; Septer *et al.*, 2011), suggesting that the light organ is a relatively low iron environment, and bacteria must acquire iron to survive. While iron plays a complex role during symbiosis and its acquisition is regulated, in part, by NO and HnoX, it remained unclear how a mutation in *hnoX* might result in more efficient colonization.

A recent report that the sensor kinase HahK functions as a positive regulator of biofilm formation (Tischler *et al.*, 2018) provided the initial insight that HnoX may function to inhibit biofilm formation. HnoX is predicted in the literature to inhibit HahK (Iyer *et al.*, 2003; Plate and Marletta, 2013), and several lines of evidence presented here support a model in which HnoX inhibits biofilm formation dependent on HahK and in response to NO (Fig. 1). An *hnoX* deletion mutant exhibits enhanced biofilm phenotypes in different genetic backgrounds and under different conditions. Enhanced biofilm phenotypes exhibited by the *hnoX* deletion mutant were most readily observed in a genetic strain background lacking known negative regulators of biofilm formation (KV7856). Utilization of this background permitted the observation of remarkable phenotypes *in vitro*, as well as a smaller but significant impact of HnoX in symbiosis. While it is possible that this strain background enhances the apparent role of HnoX, we present strong evidence that HnoX works through HahK to control biofilm formation. The precocious biofilm formation by the *hnoX* mutant was lost in the absence of HahK and was restored upon complementation with wild-type HahK but not phosphotransfer mutants. NO-mediated inhibition of pellicles and shaking cell clumping depend on the presence of HnoX, supporting the hypothesis that HnoX functions as a negative regulator of biofilm formation in response to NO. Importantly, NO also inhibits symbiotic biofilm formation (Davidson *et al.*, 2004), a result that demonstrates that the mechanisms uncovered here have biological significance during host colonization.

This study links an NO/HnoX pathway to control of production of a polysaccharide. Many HnoX proteins have been shown to interact with a downstream histidine kinase that in turn controls an adjacent diguanylate cyclase (DGC) or phosphodiesterase (PDE) (e.g. *Legionella pneumophila* (Carlson *et al.*, 2010; Liu *et al.*, 2012; Plate and Marletta, 2012)). DGC and PDE enzymes control the production and degradation of c-di-GMP, a small signaling molecule that regulates bacterial behaviors such as motility and biofilm formation (Hengge, 2009). Only two other systems have described HnoX regulatory pathways that do not appear to involve c-di-GMP: *Vibrio harveyi* and *Pseudomonas aeruginosa*. In *V. harveyi*, the HnoX protein feeds into the Lux pathway to enhance bioluminescence (Henares *et al.*, 2012). In *P. aeruginosa*, the NO-sensing protein inhibits an associated histidine kinase that facilitates phosphoryl transfer to an Hpt domain, but how the HnoX controlled phosphoryl transfer impacts phenotypes remains unknown (Hossain *et al.*, 2017). Evidence presented here suggests that in the presence of NO, HnoX inhibits transcription of the *syp* locus via HahK, resulting in decreased biofilm formation. Together, these data suggest that HnoX proteins have diverse functions in different biological pathways.

Many studies have characterized the structure of HnoX proteins and the interactions between wild-type and mutated HnoX proteins and NO. Previous work in *V. fischeri* demonstrated the ability of HnoX to bind NO (Wang *et al.*, 2010a). In *Thermoanaerobacter tengcongensis*, mutation of proline 115 to alanine increased the affinity of $HnoX_{Tt}$ for oxygen (Olea *et al.*, 2008), but the biological relevance of this mutation is unknown. In *S. woodyi*, a mutation of proline 117 to alanine in $HnoX_{So}$ had a similar effect on control over its cognate phosphodiesterase as the NO-bound wild-type $HnoX_{So}$ (Muralidharan and Boon, 2012), suggesting that the P117A mutation mimicked the NO-bound $HnoX_{So}$. Here, we show the biological relevance of a similar mutation in *V. fischeri* HnoX: the change of P114 to alanine conferred increased inhibitory activity to HnoX in biofilm formation, potentially similar to inhibition by the NO-bound HnoX. The P114A protein was still responsive to NO, however, as the addition of the NO generator inhibited biofilm formation by the P114A-containing strain, but not the Δ*hnoX* mutant. Thus, HnoX-P114A is not constitutively inhibitory and thus is unlikely to be an NO mimic. The consequence of the P114A substitution on HnoX activity will require further study.

While much is known about the structure of HnoX proteins and the interaction between HnoX proteins and NO, less is known about the interaction between HnoX proteins and their cognate partners. Several studies have shown that HnoX directly interacts with a cognate histidine kinase (e.g. $HnoX_{So}$ and HnoK in *S. oneidensis* (Price *et al.*, 2007), $HnoX_{Pa}$ and HahK in *P. atlantica* (Arora and Boon, 2012), $HnoX_{Vh}$ and HqsK in *V. harveyi* (Henares *et al.*, 2012)). In the data presented here, HahK is epistatic to HnoX in biofilm phenotypes and in transcriptional assays, suggesting that HahK and HnoX function in the same pathway. Future studies will probe the ability of HnoX to interact directly with HahK, and the sequences involved in that interaction.

Recently, calcium was identified as a signal that controls host-relevant biofilm formation by *V. fischeri* (Tischler *et al.*, 2018). While calcium is plentiful in seawater, the relevance of this signal, if any, to squid colonization is as-yet unknown. Similarly, it is unclear what evolutionary advantage is provided by the recognition of NO, the host-relevant signal we identified here, by HnoX, at least during the initial interactions with the squid: the squid secretes NO prior to and during the colonization process (Davidson *et al.*, 2004), but it (via HnoX) is detrimental to symbiotic biofilm formation (Fig. 8) and subsequent colonization (Wang *et al.*, 2010a). Given the multitude of regulators and corresponding known and unknown signals, it seems likely that *V. fischeri* integrates multiple signals to fine-tune the formation of biofilms and, subsequently, to control its ability to leave or disperse from the biofilm to enter and colonize the squid host. For example, the cells are already exposed to the positive inducer calcium when they encounter the inhibitory signal, NO. Thus, the NO/HnoX pathway may represent a fine-tuning of the effect (potentially preventing biofilms that are too adherent) and/or permit an earlier or more rapid dispersal. Alternatively, or in addition, because these signals do not act exclusively on *syp* transcription (calcium also induces cellulose production and NO controls a number of other factors, including iron uptake), *syp*-dependent biofilms represent only a subset of the responses to these signals. In either case, identifying these signals that control *syp*-dependent biofilms permit a deeper understanding of the earliest interactions between *V. fischeri* and its host.

In summary, this work identifies a host-derived signal that controls biofilm formation by *V. fischeri* and reveals the underlying regulatory pathway. This work thus paves the way for an increased mechanistic understanding of the role of HnoX proteins in controlling biologically relevant processes.

Experimental procedures

Strains and media

V. fischeri strains used in this study are listed in Table 1 and plasmids used are listed in Table 2. *V. fischeri* strains were derived by conjugation or natural transformation. *Escherichia coli* GT115 (Invivogen, San Diego, CA), π3813 (Le Roux *et al.*, 2007), Tam1 λpir, Tam1, DH5α λ*pir* and S17-1λpir were used (Simon *et al.*, 1983) for cloning and conjugation experiments (Boettcher and Ruby, 1990;

Table 1. Strains used in this study.

Strain	Genotype	Derivation[a]	Source or Reference
ES114	Wild-type		Boettcher *et al.* (1990)
KV3299	Δ*sypE sypF2*		Hussa *et al.* (2008); Thompson *et al.* (2018)
KV6439	Δ*sypEF*		Thompson *et al.* (2018)
KV6567	Δ*sypE sypF2* Δ*sypG*	Recombination using pKPQ2	This study
KV7856	Δ*binK* Δ*sypE sypF2*		Thompson *et al.* (2018)
KV7860	Δ*binK*		Tischler *et al.* (2018)
KV7952	Δ*sypE sypF2* Δ*hahK*::FRT-Em^R	NT KV3299 using PCR DNA generated with primers 2057 and 2103 (ES114), 2089 and 2090 (pKV494) and 2062 and 2104 (ES114)	This study
KV7956	Δ*binK* Δ*sypE sypF2* Δ*hahK*::FRT-Em^R	NT KV7856 with chKV7952	This study
KV8025	Δ*hnoX*::FRT-Em^R	NT KV3299 using PCR DNA generated with primers 2155 and 2156 (ES114), 2089 and 2090 (pKV494) and 2057 and 2158 (ES114)	This study
KV8027	Δ*sypE sypF2* Δ*hnoX*::FRT-Em^R	NT KV3299 using PCR DNA generated with primers 2155 and 2156 (ES114), 2089 and 2090 (pKV494) and 2057 and 2158 (ES114)	This study
KV8032	Δ*binK* Δ*sypE sypF2* Δ*hnoX*::FRT-Em^R	NT KV7856 with chKV8025	This study
KV8055	Δ*binK* Δ*sypEF*		Thompson *et al.* (2018)
KV8135	IG (*yeiR-glmS*)::FRT-Em^R-*hnoX-HA*	NT ES114 using PCR DNA generated with primers 2185 and 2090 (pKV502), 2196 and 1487 (pKV505) and 2207 and 2208 (ES114)	This study
KV8136	IG (*yeiR-glmS*)::FRT-Em^R-*hnoX-P115A-HA*	NT ES114 using PCR DNA generated with primers 2185 and 2090 (pKV502), 2196 and 1487 (pKV505) and 2207 and 2208 (pKV525)	This study
KV8137	IG (*yeiR-glmS*)::FRT-Em^R-*hnoX-P114A-HA*	NT ES114 using PCR DNA generated with primers 2185 and 2090 (pKV502), 2196 and 1487 (pKV505) and 2207 and 2208 (pCMT34)	This study
KV8150	Δ*binK* Δ*sypE sypF2* Δ*hnoX*::FRT	Removal of Em^R cassette from KV8032 with Flp (pKV496)	This study
KV8175	Δ*binK* Δ*sypE sypF2* Δ*hnoX*::FRT IG (*yeiR-glmS*)::FRT-Em^R-*hnoX-HA*	NT KV8150 with chKV8135	This study
KV8176	Δ*binK* Δ*sypE sypF2* Δ*hnoX*::FRT IG (*yeiR-glmS*)::FRT-Em^R-*hnoX-P115A-HA*	NT KV8150 with chKV8136	This study
KV8177	Δ*binK* Δ*sypE sypF2* Δ*hnoX*::FRT IG (*yeiR-glmS*)::FRT-Em^R-*hnoX-P114A-HA*	NT KV8150 with chKV8137	This study
KV8232	IG (*yeiR-glmS*)::Erm-trunc-Tm^R		Visick *et al.* (2018)
KV8237	IG (*yeiR-glmS*)::FRT-Em^R-*hahK-HA*	NT KV8232 using PCR DNA generated with primers 2290 and 2090 (pKV506), 2201 and 2202 (pKV522) and 2196 and 1487 (pKV503)	This study
KV8238	IG (*yeiR-glmS*)::FRT-Em^R-*hahK-H222Q-HA*	NT KV8232 using PCR DNA generated with primers 2290 and 2090 (pKV506), 2201 and 2202 (pKV523) and 2196 and 1487 (pKV503)	This study
KV8250	IG (*yeiR-glmS*)::FRT-Em^R-*hahK-D506A-HA*	NT KV8232 using PCR DNA generated with primers 2290 and 2090 (pKV506), 2201 and 2202 (pKV524) and 2196 and 1487 (pKV503)	This study
KV8310	Δ*binK* Δ*hnoX*::FRT	Removal of Em cassette from KV8538 with Flp (pKV496)	This study
KV8458	Δ*binK*::FRT-Tm^R	NT ES114 using PCR DNA generated with primers 1268 and 2091 (ES114), 2089 and 2090 (pMLC2) and 2092 and 1271 (ES114)	This study
KV8484	Δ*hnoX-hahK*::FRT-Em^R	NT ES114 using PCR DNA generated with primers 2207 and 2292 (KV8025) and 2290 and 2103 (KV7952)	This study
KV8485	Δ*binK* Δ*sypE sypF2* Δ(*hnoX-hahK)*::FRT-Em^R	NT KV7856 with chKV8484	This study

(Continued)

Table 1. *Continued*

Strain	Genotype	Derivation[a]	Source or Reference
KV8486	Δ*binK* Δ*sypE sypF2* Δ*hnoX-hahK*::FRT *att*Tn*7*::*hnoX-hahK*	Derived from KV8493 using pLL8	This study
KV8487	Δ*binK* Δ*sypE sypF2* IG (*yeiR-glmS*)::FRT-Em^R-*hnoX-P114A-HA*	NT KV7856 with chKV8137	This study
KV8489	Δ*binK* Δ*hnoX*::FRT IG (*yeiR-glmS*)::FRT-Em^R-*hnoX-HA*	NT KV7860 with chKV8135	This study
KV8492	Δ*binK* Δ*sypE sypF2* IG (*yeiR-glmS*)::FRT-Em^R-*hnoX-HA*	NT KV7856 with chKV8135	This study
KV8493	Δ*binK* Δ*sypE sypF2* Δ*hnoX-hahK*::FRT	Removal of Em cassette from KV8485 with Flp (pKV496)	This study
KV8494	Δ*binK* Δ*sypE sypF2* Δ*hnoX-hahK*::FRT IG (*yeiR-glmS*)::FRT-Em^R-*hnoX-HA*	NT KV8493 with chKV8135	This study
KV8500	Δ*binK* Δ*sypE sypF2* Δ*hnoX*::FRT IG (*yeiR-glmS*)::FRT-Em^R-*hahK-HA*	NT KV8150 with chKV8237	This study
KV8501	Δ*binK* Δ*sypE sypF2* Δ*hnoX*::FRT IG (*yeiR-glmS*)::FRT-Em^R-*hahK-D506A-HA*	NT KV8150 with chKV8238	This study
KV8502	Δ*binK* Δ*sypE sypF2* Δ*hnoX*::FRT IG (*yeiR-glmS*)::FRT-Em^R-*hahK-H222Q-HA*	NT KV8150 with chKV8250	This study
KV8503	Δ*binK* Δ*sypE sypF2* Δ*hnoX-hahK*::FRT IG(*yeiR-glmS*)::FRT-Em^R-*hahK-D506A-HA*	NT KV8493 with chKV8238	This study
KV8504	Δ*binK* Δ*sypE sypF2* Δ*hnoX-hahK*::FRT IG(*yeiR-glmS*)::FRT-Em^R-*hahK-H222Q-HA*	NT KV8493 with chKV8250	This study
KV8507	Δ*binK* Δ*sypE sypF2* Δ*hnoX-hahK*::FRT IG (*yeiR-glmS*)::FRT-Em^R-*hahK-HA*	NT KV8493 with chKV8237	This study
KV8538	Δ*binK* Δ*hnoX*::FRT-Em^R	NT KV7860 with chKV8025	This study
KV8607	Δ*sypE sypF2* Δ*sypG* Δ*binK*::FRT- Tm^R	NT KV6567 with chKV8458	This study
KV8611	Δ*sypE sypF2* Δ*sypG* Δ*binK*::FRT- Tm^R Δ*hnoX*::FRT-Em^R	NT KV8607 with chKV8025	This study

[a]Derivation of strains constructed in this study; NT, natural transformation of a pLostfoX or pLostfoX-Kan-carrying version of the strain with the indicated chromosomal (ch) DNA or with a PCR SOE product generated using the indicated primers and templates (in parentheses). IG, intergenic region between the genes indicated in parentheses.

Visick and Skoufos, 2001). *V. fischeri* strains were cultured in Luria-Bertani salt (LBS) medium (Stabb *et al.*, 2001). The following antibiotics were added to LBS medium at the indicated concentrations: chloramphenicol (Cm) at 1 or 2.5 μg ml^{-1}, erythromycin (Em) at 2.5 μg ml^{-1}, kanamycin (Kan) at 100 μg ml^{-1}, trimethoprim (Tm) at 10 μg ml^{-1} and tetracycline (Tc) at 2.5 μg ml^{-1}. *E. coli* strains were cultured in the Luria-Bertani medium (LB) (Davis *et al.*, 1980) containing 10 g Bacto-Tryptone, 5 g yeast extract and 10 g NaCl per liter. The following antibiotics were added to the LB medium at the indicated concentrations: Kan at 50 μg ml^{-1}, Tc at 15 μg ml^{-1} or ampicillin (Ap) at 100 μg ml^{-1}. For solid media, agar was added to a final concentration of 1.5%.

Because wild-type strain ES114 does not form *syp*-dependent biofilms under standard laboratory conditions, strain KV7856 was used as the parent for most of the experiments in this work. This strain contains mutations in three negative regulators, *binK*, *sypE* and *sypF* (Δ*binK* Δ*sypE sypF2*). Together, these mutations disrupt the extensive negative control that *V. fischeri* exerts over biofilm formation while still permitting the positive regulation provided by SypF (the *sypF2* allele disrupts the negative function of SypF while retaining its critical positive activity). This strain is competent to produce wrinkled colonies and pellicles in the absence of a plasmid-based overexpression of positive regulators and in the absence of the inducing signal calcium (Thompson *et al.*, 2018), and thus provides a tool for readily evaluating other regulatory inputs.

Bioinformatics

Sequences for *V. fischeri hnoX* (*VF_A0071*) and *hahK* (*VF_A0072*) were obtained from the National Center for Biotechnology Information (NCBI) database. Alignments were generated using BLAST and the Clustal Omega multiple-sequence alignment program from EMBL-EBI (https://www.ebi.ac.uk/Tools/msa/clustalw2/) (Altschul *et al.*, 1997; 2005; Larkin *et al.*, 2007; Sievers *et al.*, 2011).

Molecular and genetic techniques

Derivatives of *V. fischeri* were generated via conjugation (DeLoney *et al.*, 2002) or transformation (Pollack-Berti *et al.*, 2010; Brooks *et al.*, 2014). Some constructs were pEVS107-based and were inserted into the chromosomal Tn*7* site of *V. fischeri* strains using tetraparental conjugation (McCann *et al.*, 2003). Deletion of *sypG* was generated using the arabinose-inducible toxin-based approach of Le Roux (Le Roux *et al.*, 2007) with plasmid pKPQ2. Plasmid pKPQ2 was derived using PCR SOEing (Splicing by Overlap Extension) (Ho *et al.*, 1989) using primers 1223, 1221, 1222 and 427. For the remainder of the genetic

Table 2. Plasmids used in this study.

Plasmid	Description[a]	Source or Reference
pANN50	pEVS107 + P_{lac} *sypF*-Hpt	Norsworthy and Visick (2015)
pARM131	pEVS107 + P_{sypA} *sypA*	Morris and Visick (2013b)
pCMT34	pJET + *hnoX-P114A-HA*	This study
pEVS104	Conjugal plasmid	Stabb and Ruby (2002)
pEVS107	Tn*7* delivery plasmid, Em^R Km^R	McCann *et al.* (2003)
pEVS170	Vector containing Em^R, Km^R	Lyell *et al.* (2008)
pJET1.2/blunt	Commercial cloning vector, Ap^R	Thermofisher
pKPQ2	pKV363 + sequences flanking *sypG*	This study
pKV282	Low copy vector, Tc^R	Morris *et al.* (2011)
pKV494	pJET + FRT-Em^R	Visick *et al.* (2018)
pKV495	pJET + FRT-Cm^R	Visick *et al.* (2018)
pKV496	pJET + Flp recombinase	Visick *et al.* (2018)
pKV503	pJET + *glmS*	Visick *et al.* (2018)
pKV505	pJET + *HA-glmS*	Visick *et al.* (2018)
pKV506	pJET + *yeiR*-FRT-Em^R-P*nrdR*	Visick *et al.* (2018)
pKV522	pJET + *hahK-HA*	This study
pKV523	pJET + *hahK-H222Q-HA*	This study
pKV524	pJET + *hahK-D506A-HA*	This study
pKV525	pJET + *hnoX-P115A-HA*	This study
pLL3	pVSV209 + P*sypA-GFP*	This study
pLL8	pEVS107 + *hnoX-hahK*	This study
pLosTfoX	Expresses TfoX, Cm^R	Pollack-Berti *et al.* (2010)
pLostfoX-Kan	Expresses TfoX, Km^R	Brooks *et al.* (2014)
pMLC2	pJET + Tm^R	Visick *et al.* (2018)
pUX-BF13	Tn*7* transposase expressing vector	Bao *et al.* (1991)
pVSV102	Constitutive GFP expression vector	Dunn *et al.* (2006)
pVSV209	Promoterless GFP vector	Dunn *et al.* (2006)

[a]Details on construction are included for plasmids generated in this study; ES114 was used as a template for PCR reactions.

engineering procedures, the methods of (Visick *et al.*, 2018) were used to generate marked and unmarked deletions, complementation constructs and point mutations. Specifically, the *hnoX* and *hahK* alleles used in this study were generated, and, in some cases, HA epitope-tagged, by Polymerase Chain Reaction (PCR) or PCR SOEing using primers listed in Table 3 and EMD Millipore Novagen KOD high fidelity polymerase. To generate deletions, sequences (~500 bp) upstream and downstream of the gene of interest were amplified by PCR, then fused with an antibiotic resistance cassette in a PCR SOEing reaction. The final spliced PCR product was introduced into *tfoX*-overexpressing ES114 by transformation. Recombination of the PCR product into the chromosome producing the desired gene replacement mutant was selected using the antibiotic resistance marker. Promega Taq was used to confirm gene replacement events. A similar approach was used to introduce complementation or expression cassettes adjacent to the Tn*7* site (in the intergenic region between *yeiR* and *glmS* (IG(*yeiR-glmS*)) as described (Visick *et al.*, 2018). To generate the *hahK* and *hnoX* point mutants, the following primer sets were used for PCR to generate a DNA fragment that was cloned into pJET, sequenced and subsequently used as a template for PCR SOEing to fuse the flanking DNA for insertion at IG (y*eiR-glmS*): 2152, 2177, 2176 and 2180 (*hahK*-H222Q; pKV523), 2152, 2179, 2178 and 2180 (*hahK*-D506A; pKV524), 2207, 2210, 2209 and 2208 (*hnoX*-P115A; pKV525) and 2207, 2302, 2303 and 2208 (*hnoX*-P114A; pCMT34). Chromosomal DNA was isolated from ES114 recombinants using the DNeasy Blood & Tissue Kit (Qiagen) or Quick-DNA Microprep Kit (Zymogen). Sequencing reactions were performed by ACGT, Inc. (Wheeling, IL).

Wrinkled colony formation assay

The indicated *V. fischeri* strains were streaked onto LBS agar plates. Single colonies were then cultured with shaking in 5 ml LBS broth overnight at 28°C. The strains were then subcultured the following day in 5 ml of fresh medium. Following growth to early log phase, the cultures were standardized to an optical density at 600 nm (OD_{600}) of 0.2 using LBS. Ten microlitres of diluted cultures were spotted onto LBS agar plates and grown at 24°C. Images of the spotted cultures were acquired over the course of wrinkled colony formation at the indicated times using a Zeiss Stemi 2000-C dissecting microscope and Jenoptik PROGRES GRYPHAX® series SUBRA camera. All images were taken at the same magnification, and scale bars indicate 200 µm. At the end of the time course, the colonies were disrupted with a toothpick to assess colony cohesiveness, which is an indicator of Syp production (Ray *et al.*, 2015).

Pellicle formation assay

V. fischeri strains were grown overnight and subcultured with shaking as described above. Following growth to mid-log phase, the cultures were standardized to an optical density

Table 3. Primers.

Primer	Sequence (5′–3′)[a]
427	TAATACCGTTGTTTTGCTTGG
1221	taggcggccgcacttagtatggTCTTCGACTAATAATACTTTCTG
1222	catactaagtgcggccgcctaGAAGCCTATGAAGAATCGGAATGATG
1223	GAATGTCTTGCTAAGTACCTG
1268	GGAGCCAACAGCAAGACTTA
1271	TGCCACCGTTTCTCGTGTAG
1487	GGTCGTGGGGAGTTTTATCC
2009	gggtctttttgcatgccctaggAGCTTCTTCCTTATAGTTATGATG
2010	tcctagctaggcctgtcgacTAGGGAATAATCCTCGTTGTTTC
2057	CCTTATCTGTACGAGTATTGG
2062	ATTCATCTTAACTGCGATCGC
2089	CCATACTTAGTGCGGCCGCCTA
2090	CCATGGCCTTCTAGGCCTATCC
2091	taggcggccgcactaagtatggATAGCAAGCTAACGCGAGAATGC
2092	ggataggcctagaaggccatggTTGGAAGCGTATACATAAATAATGATTC
2103	taggcggccgcactaagtatggATCAACATCCATTTATCCCGC
2104	ggataggcctagaaggccatggGCAATGTTAAAGCTTTGGGGT
2152	gcatgcCGATTAAGGCGGGATAAATG
2153	gggcccCCTCGCAATATTGTGAGGC
2154	actagtTAATTATGGAAGCGAGTGCAG
2155	ATCTCTTGAGCACTTGTTTGAG
2156	taggcggccgcactaagtatggAATAATCCCTTTCATAAACACTCC
2157	ggataggcctagaaggccatggAAATCATAAACGATTAAGGCGGG
2158	TCGCGCCACATTGTATTTGG
2176	TGATAAACCAgGAATTAAGAACACCATTAAATG
2177	TTCTTAATTCcTGGTTTATCATCGCAACGAAG
2178	GTTTTAATGGcTTGTCGAATGCCGATTCTTG
2179	CATTCGACAAgCCATTAAAACAATATCAA
2180	ttatgcataatctggaacatcatatggataTACATACTTAGAACCCCAAAGCTTTAAC
2185	CTTGATTTATACAGCGAAGGAG
2196	TCCATACTTAGTGCGGCCGCCTA
2201	ggataggcctagaaggccatggCGATTAAGGCGGGATAAATG
2202	taggcggccgcactaagtatggATTATGCATAATCTGGAACATCATATGG
2207	ggataggcctagaaggccatggTAATTATGGAAGCGAGTGCAG
2208	taggcggccgcactaagtatggATGATTTAGTTAAGGTAAAACGAAC
2209	AGCGAACCCTgCGCGTTTTAAGTTTATATC
2210	TTAAAACGCGcAGGGTTCGCTTCAGCGTATAAC
2290	AAGAAACCGATACCGTTTACG
2292	gctgatgcttaccgttaattaattaGGCGTGTTTCATTGCTTGATG
2302	CTGAAGCGAACgCTCCGCGTTTTAAGTTTATA
2303	AAACGCGGAGcGTTCGCTTCAGCGTATAACT

[a]Lowercase letters indicate non-native sequences or 'tails' added to the PCR product that were not complementary to the target DNA.

at 600 nm (OD_{600}) of 0.2 using LBS in 24-well microtiter plates. Inoculated microtiter plates were incubated statically at 24°C. Images of the microtiter wells were acquired over the course of pellicle formation at the indicated times using a Zeiss Stemi 2000-C dissecting microscope and Jenoptik PROGRES GRYPHAX® series SUBRA camera. At the end of the time course, the pellicles were disrupted with a toothpick to evaluate pellicle strength.

Cell clumping assay

Single colonies of *V. fischeri* strains were inoculated in 13 × 100 mm test tubes containing 2 ml LBS liquid media with and without the addition of 10 mM calcium chloride. Cultures were incubated at 24°C. Images of the cultures were acquired at the indicated time using an iPhone 7 camera.

NO generator preparation

In biofilm assays, the cells were exposed to Diethylenetriamine (DETA)-NONOate (Cayman Chemical), an NO generator with a half-life of 56 h at 22–25°C. A stock solution of 100 mM was prepared by reconstituting DETA-NONOate in water immediately before use. From the stock solution, dilutions were made as indicated into 2 ml of culture for pellicle assays or shaking cell clumping assays. For transcription experiments, strains were exposed to 500 µM Dipropylenetriamine (DPTA)-NONOate (Cayman Chemical), which has a half-life of 5 h at 22–25°C.

Transcriptional reporter assay

Strains of *V. fischeri* carrying a plasmid-based P*sypA-GFP* reporter were cultured overnight in duplicate in an *N*-acetylglucosamine-based minimal medium. The next

day, strains were subcultured; the strains were transferred into fresh media at an OD_{600} = 0.05 and grown at 24°C for 3 h. When testing the response to NO, half of the cultures were exposed to 500 μM DPTA-NONOate (Fig. 6B) while the other half were not exposed (Fig. 6A). The levels of *syp* transcription were measured over time using fluorescence (arbitrary units) per cell (per optical density (OD_{600})) as a read-out for transcription using a Synergy H1 microplate reader (BioTek). Fluorescence per cell was normalized to the background transcription induction of a biofilm-deficient strain, which is indicated by a dotted line. Graphed data are from at least three independent experiments. Error bars indicate standard deviation. The data were analyzed using a two-way ANOVA (Fig. 6A and D) and a one-way ANOVA (Fig. 6B and C) using Graphpad Prism 6.

Aggregation experiments

Juvenile *E. scolopes* were collected within 12 h of hatching and incubated with approximately 3×10^6 bacteria containing GFP-encoding plasmid pVSV102 for three hours at room temperature in filter-sterilized instant ocean. Squid were anesthetized in 2% ethanol and dissected to expose the light organ using a Leica EZ4 stereomicroscope. Aggregates were visualized on a Zeiss AxioZoom V16 microscope and measured using Zeiss ZEN Blue software. Bacterial colonies from inoculum seawater samples were visualized to confirm the expression of GFP. The data were analyzed using a Mann-Whitney test on Graphpad Prism 6.

Acknowledgements

We thank Allison Norsworthy, Louise Lie, Kevin Quirke and Kelsey Hodge-Hanson for strain and plasmid construction, and members of the lab for thoughtful discussions and review of the manuscript. This work was supported by NIH grant R01 GM114288 awarded to K.L.V., R35 GM119627 and R21 AI117262 awarded to M.J.M. and NSF grant IOS-1757297 awarded to M.J.M.

References

Altschul, S.F., Madden, T.L., Schaffer, A.A., Zhang, J., Zhang, Z., Miller, W., *et al.* (1997) Gapped BLAST and PSI-BLAST: a new generation of protein database search programs. *Nucleic Acids Research*, **25**, 3389–3402.

Altschul, S.F., Wootton, J.C., Gertz, E.M., Agarwala, R., Morgulis, A., Schaffer, A.A., *et al.* (2005) Protein database searches using compositionally adjusted substitution matrices. *FEBS Journal*, **272**, 5101–5109.

Arora, D.P. and Boon, E.M. (2012) Nitric oxide regulated two-component signaling in *Pseudoalteromonas atlantica*. *Biochemical and Biophysical Research Communications*, **421**, 521–526.

Bao, Y., Lies, D.P., Fu, H. and Roberts, G.P. (1991) An improved Tn*7*-based system for the single-copy insertion of cloned genes into chromosomes of gram-negative bacteria. *Gene*, **109**, 167–168.

Boettcher, K.J. and Ruby, E.G. (1990) Depressed light emission by symbiotic *Vibrio fischeri* of the sepiolid squid *Euprymna scolopes*. *Journal of Bacteriology*, **172**, 3701–3706.

Brooks, J.F. 2nd, Gyllborg, M.C., Cronin, D.C., Quillin, S.J., Mallama, C.A., Foxall, R., *et al.* (2014) Global discovery of colonization determinants in the squid symbiont *Vibrio fischeri*. *Proceedings of the National Academy of Sciences of the United States of America*, **111**, 17284–17289.

Brooks, J.F. 2nd and Mandel, M.J. (2016) The histidine kinase BinK is a negative regulator of biofilm formation and squid colonization. *Journal of Bacteriology*, **198**, 2596–2607.

Carlson, H.K., Vance, R.E. and Marletta, M.A. (2010) H-NOX regulation of c-di-GMP metabolism and biofilm formation in *Legionella pneumophila*. *Molecular Microbiology*, **77**, 930–942.

Crane, B.R., Sudhamsu, J. and Patel, B.A. (2010) Bacterial nitric oxide synthases. *Annual Review of Biochemistry*, **79**, 445–470.

Davidson, S.K., Koropatnick, T.A., Kossmehl, R., Sycuro, L. and McFall-Ngai, M.J. (2004) NO means 'yes' in the squid-vibrio symbiosis: nitric oxide (NO) during the initial stages of a beneficial association. *Cell Microbiology*, **6**, 1139–1151.

Davis, R.W., Botstein, D., Roth, J.R. and Cold Spring Harbor Laboratory. (1980) *Advanced Bacterial Genetics*. Cold Spring Harbor, NY: Cold Spring Harbor Laboratory.

DeLoney, C.R., Bartley, T.M. and Visick, K.L. (2002) Role for phosphoglucomutase in *Vibrio fischeri-Euprymna scolopes* symbiosis. *Journal of Bacteriology*, **184**, 5121–5129.

Derbyshire, E.R. and Marletta, M.A. (2009) Biochemistry of soluble guanylate cyclase. *Handbook of Experimental Pharmacology*, **191**, 17–31.

Dunn, A.K., Millikan, D.S., Adin, D.M., Bose, J.L. and Stabb, E.V. (2006) New *rfp*- and pES213-derived tools for analyzing symbiotic *Vibrio fischeri* reveal patterns of infection and *lux* expression in situ. *Applied and Environmental Microbiology*, **72**, 802–810.

Fang, F.C. (2004) Antimicrobial reactive oxygen and nitrogen species: concepts and controversies. *Nature Reviews Microbiology*, **2**, 820–832.

Gardner, A.M., Gessner, C.R. and Gardner, P.R. (2003) Regulation of the nitric oxide reduction operon (*norRVW*) in *Escherichia coli*. Role of NorR and σ54 in the nitric oxide stress response. *Journal of Biological Chemistry*, **278**, 10081–10086.

Gardner, A.M., Helmick, R.A. and Gardner, P.R. (2002) Flavorubredoxin, an inducible catalyst for nitric oxide reduction and detoxification in *Escherichia coli*. *Journal of Biological Chemistry*, **277**, 8172–8177.

Graf, J., Dunlap, P.V. and Ruby, E.G. (1994) Effect of transposon-induced motility mutations on colonization of the host light organ by *Vibrio fischeri*. *Journal of Bacteriology*, **176**, 6986–6991.

Henares, B.M., Higgins, K.E. and Boon, E.M. (2012) Discovery of a nitric oxide responsive quorum sensing circuit in *Vibrio harveyi*. *ACS Chemical Biology*, **7**, 1331–1336.

Henares, B.M., Xu, Y. and Boon, E.M. (2013) A nitric oxide-responsive quorum sensing circuit in *Vibrio harveyi* regulates flagella production and biofilm formation. *International Journal of Molecular Sciences*, **14**, 16473–16484.

Hengge, R. (2009) Principles of c-di-GMP signalling in bacteria. *Nature Reviews Microbiology*, **7**, 263–273.

Ho, S.N., Hunt, H.D., Horton, R.M., Pullen, J.K. and Pease, L.R. (1989) Site-directed mutagenesis by overlap extension using the polymerase chain reaction. *Gene*, **77**, 51–59.

Hossain, S. and Boon, E.M. (2017) Discovery of a novel nitric oxide binding protein and nitric-oxide-responsive signaling pathway in *Pseudomonas aeruginosa*. *ACS Infectious Diseases*, **3**, 454–461.

Hussa, E.A., Darnell, C.L. and Visick, K.L. (2008) RscS functions upstream of SypG to control the *syp* locus and biofilm formation in *Vibrio fischeri*. *Journal of Bacteriology*, **190**, 4576–4583.

Hussa, E.A., O'Shea, T.M., Darnell, C.L., Ruby, E.G. and Visick, K.L. (2007) Two-component response regulators of *Vibrio fischeri*: identification, mutagenesis, and characterization. *Journal of Bacteriology*, **189**, 5825–5838.

Iyer, L.M., Anantharaman, V. and Aravind, L. (2003) Ancient conserved domains shared by animal soluble guanylyl cyclases and bacterial signaling proteins. *BMC Genomics*, **4**, 5.

Larkin, M.A., Blackshields, G., Brown, N.P., Chenna, R., McGettigan, P.A., McWilliam, H., *et al.* (2007) Clustal W and Clustal X version 2.0. *Bioinformatics*, **23**, 2947–2948.

Le Roux, F., Binesse, J., Saulnier, D. and Mazel, D. (2007) Construction of a *Vibrio splendidus* mutant lacking the metalloprotease gene vsm by use of a novel counterselectable suicide vector. *Applied and Environmental Microbiology*, **73**, 777–784.

Liu, N., Xu, Y., Hossain, S., Huang, N., Coursolle, D., Gralnick, J.A., *et al.* (2012) Nitric oxide regulation of cyclic di-GMP synthesis and hydrolysis in *Shewanella woodyi*. *Biochemistry*, **51**, 2087–2099.

Lyell, N.L., Dunn, A.K., Bose, J.L., Vescovi, S.L. and Stabb, E.V. (2008) Effective mutagenesis of *Vibrio fischeri* by using hyperactive mini-Tn5 derivatives. *Applied and Environmental Microbiology*, **74**, 7059–7063.

McCann, J., Stabb, E.V., Millikan, D.S. and Ruby, E.G. (2003) Population dynamics of *Vibrio fischeri* during infection of *Euprymna scolopes*. *Applied and Environmental Microbiology*, **69**, 5928–5934.

Morris, A.R., Darnell, C.L. and Visick, K.L. (2011) Inactivation of a novel response regulator is necessary for biofilm formation and host colonization by *Vibrio fischeri*. *Molecular Microbiology*, **82**, 114–130.

Morris, A.R. and Visick, K.L. (2013a) Inhibition of SypG-induced biofilms and host colonization by the negative regulator SypE in *Vibrio fischeri*. *PLoS One*, **8**, e60076.

Morris, A.R. and Visick, K.L. (2013b) The response regulator SypE controls biofilm formation and colonization through phosphorylation of the *syp*-encoded regulator SypA in *Vibrio fischeri*. *Molecular Microbiology*, **87**, 509–525.

Muralidharan, S. and Boon, E.M. (2012) Heme flattening is sufficient for signal transduction in the H-NOX family. *Journal of the American Chemical Society*, **134**, 2044–2046.

Norsworthy, A.N. and Visick, K.L. (2015) Signaling between two interacting sensor kinases promotes biofilms and colonization by a bacterial symbiont. *Molecular Microbiology*, **96**, 233–248.

Nyholm, S.V., Deplancke, B., Gaskins, H.R., Apicella, M.A. and McFall-Ngai, M.J. (2002) Roles of *Vibrio fischeri* and nonsymbiotic bacteria in the dynamics of mucus secretion during symbiont colonization of the *Euprymna scolopes* light organ. *Applied and Environmental Microbiology*, **68**, 5113–5122.

Nyholm, S.V., Stabb, E.V., Ruby, E.G. and McFall-Ngai, M.J. (2000) Establishment of an animal-bacterial association: recruiting symbiotic vibrios from the environment. *Proceedings of the National Academy of Sciences of the United States of America*, **97**, 10231–10235.

Olea, C., Boon, E.M., Pellicena, P., Kuriyan, J. and Marletta, M.A. (2008) Probing the function of heme distortion in the H-NOX family. *ACS Chemical Biology*, **3**, 703–710.

Pankey, S.M., Foxall, R.L., Ster, I.M., Perry, L.A., Schuster, B.M., Donner, R.A., *et al.* (2017). Host-selected mutations converging on a global regulator drive an adaptive leap towards symbiosis in bacteria. *Elife*, **6**, e24414.

Plate, L. and Marletta, M.A. (2012) Nitric oxide modulates bacterial biofilm formation through a multicomponent cyclic-di-GMP signaling network. *Molecular Cell*, **46**, 449–460.

Plate, L. and Marletta, M.A. (2013) Nitric oxide-sensing H-NOX proteins govern bacterial communal behavior. *Trends in Biochemical Sciences*, **38**, 566–575.

Pollack-Berti, A., Wollenberg, M.S. and Ruby, E.G. (2010) Natural transformation of *Vibrio fischeri* requires *tfoX* and *tfoY*. *Environmental Microbiology*, **12**, 2302–2311.

Poock, S.R., Leach, E.R., Moir, J.W., Cole, J.A. and Richardson, D.J. (2002) Respiratory detoxification of nitric oxide by the cytochrome c nitrite reductase of *Escherichia coli*. *Journal of Biological Chemistry*, **277**, 23664–23669.

Poole, R.K., Anjum, M.F., Membrillo-Hernandez, J., Kim, S.O., Hughes, M.N. and Stewart, V. (1996) Nitric oxide, nitrite, and Fnr regulation of *hmp* (flavohemoglobin) gene expression in *Escherichia coli* K-12. *Journal of Bacteriology*, **178**, 5487–5492.

Price, M.S., Chao, L.Y. and Marletta, M.A. (2007) *Shewanella oneidensis* MR-1 H-NOX regulation of a histidine kinase by nitric oxide. *Biochemistry*, **46**, 13677–13683.

Ray, V.A., Driks, A. and Visick, K.L. (2015) Identification of a novel matrix protein that promotes biofilm maturation in *Vibrio fischeri*. *Journal of Bacteriology*, **197**, 518–528.

Ray, V.A., Eddy, J.L., Hussa, E.A., Misale, M. and Visick, K.L. (2013) The *syp* enhancer sequence plays a key role in transcriptional activation by the σ54-dependent response regulator SypG and in biofilm formation and host colonization by *Vibrio fischeri*. *Journal of Bacteriology*, **195**, 5402–5412.

Reiter, T.A. (2006) NO* chemistry: a diversity of targets in the cell. *Redox Report*, **11**, 194–206.

Septer, A.N., Wang, Y., Ruby, E.G., Stabb, E.V. and Dunn, A.K. (2011) The haem-uptake gene cluster in *Vibrio fischeri* is regulated by Fur and contributes to symbiotic colonization. *Environmental Microbiology*, **13**, 2855–2864.

Shibata, S., Yip, E.S., Quirke, K.P., Ondrey, J.M. and Visick, K.L. (2012) Roles of the structural symbiosis

polysaccharide (*syp*) genes in host colonization, biofilm formation, and polysaccharide biosynthesis in *Vibrio fischeri*. *Journal of Bacteriology*, **194**, 6736–6747.
Sievers, F., Wilm, A., Dineen, D., Gibson, T.J., Karplus, K., Li, W., *et al.* (2011) Fast, scalable generation of high-quality protein multiple sequence alignments using Clustal Omega. *Molecular Systems Biology*, **7**, 539.
Simon, R., Priefer, U. and Pühler, A. (1983) A broad host range mobilization system for *in vivo* genetic engineering: transposon mutagenesis in Gram negative bacteria. *Bio/Technology*, **1**, 784–791.
Spiro, S. (2007) Regulators of bacterial responses to nitric oxide. *FEMS Microbiology Reviews*, **31**, 193–211.
Stabb, E.V., Reich, K.A. and Ruby, E.G. (2001) *Vibrio fischeri* genes *hvnA* and *hvnB* encode secreted NAD(+)-glycohydrolases. *Journal of Bacteriology*, **183**, 309–317.
Stabb, E.V. and Ruby, E.G. (2002) RP4-based plasmids for conjugation between *Escherichia coli* and members of the *Vibrionaceae*. *Methods in Enzymology*, **358**, 413–426.
Stevanin, T.M., Poole, R.K., Demoncheaux, E.A. and Read, R.C. (2002) Flavohemoglobin Hmp protects *Salmonella enterica* serovar *typhimurium* from nitric oxide-related killing by human macrophages. *Infection and Immunity*, **70**, 4399–4405.
Thompson, C.M., Marsden, A.E., Tischler, A.H., Koo, J. and Visick, K.L. (2018) *Vibrio fischeri* biofilm formation prevented by a trio of regulators. *Applied and Environmental Microbiology*, **84**, e01257-18.
Tischler, A.H., Lie, L., Thompson, C.M. and Visick, K.L. (2018) Discovery of calcium as a biofilm-promoting signal for *Vibrio fischeri* reveals new phenotypes and underlying regulatory complexity. *Journal of Bacteriology*, **200**, e00016-18.
Visick, K.L. (2009) An intricate network of regulators controls biofilm formation and colonization by *Vibrio fischeri*. *Molecular Microbiology*, **74**, 782–789.
Visick, K.L., Hodge-Hanson, K.M., Tischler, A.H., Bennett, A.K. and Mastrodomenico, V. (2018) Tools for rapid genetic engineering of *Vibrio fischeri*. *Applied and Environmental Microbiology*, **84**, e00850-18.
Visick, K.L. and Skoufos, L.M. (2001) Two-component sensor required for normal symbiotic colonization of *Euprymna scolopes* by *Vibrio fischeri*. *Journal of Bacteriology*, **183**, 835–842.
Wang, Y., Dufour, Y.S., Carlson, H.K., Donohue, T.J., Marletta, M.A. and Ruby, E.G. (2010a) H-NOX-mediated nitric oxide sensing modulates symbiotic colonization by *Vibrio fischeri*. *Proceedings of the National Academy of Sciences of the United States of America*, **107**, 8375–8380.
Wang, Y., Dunn, A.K., Wilneff, J., McFall-Ngai, M.J., Spiro, S. and Ruby, E.G. (2010b) *Vibrio fischeri* flavohaemoglobin protects against nitric oxide during initiation of the squid-Vibrio symbiosis. *Molecular Microbiology*, **78**, 903–915.
Yip, E.S., Geszvain, K., DeLoney-Marino, C.R. and Visick, K.L. (2006) The symbiosis regulator RscS controls the *syp* gene locus, biofilm formation and symbiotic aggregation by *Vibrio fischeri*. *Molecular Microbiology*, **62**, 1586–1600.

Supporting Information

Additional supporting information may be found online in the Supporting Information section at the end of the article.